Journal of Catalysis 272 (2010) 65–73

Contents lists available at ScienceDirect

Journal of Catalysis

journal homepage: www.elsevier.com/locate/jcat

Efficient and stable silica-supported iron phosphate catalysts for oxidative bromination of methane

Ronghe Lin [a,c], Yunjie Ding [a,b,*], Leifeng Gong [a,c], Wenda Dong [a,c], Junhu Wang [b], Tao Zhang [b,**]

[a] Dalian National Laboratory for Clean Energy, Dalian Institute of Chemical Physics, Chinese Academy of Sciences, Dalian 116023, PR China
[b] State Key Laboratory of Catalysis, Dalian Institute of Chemical Physics, Chinese Academy of Sciences, Dalian 116023, PR China
[c] Graduate School of Chinese Academy of Sciences, Beijing 100049, PR China

ARTICLE INFO

Article history:
Received 26 January 2010
Revised 8 March 2010
Accepted 10 March 2010
Available online 8 April 2010

Keywords:
Methane
Oxidative bromination
Iron phosphate
CH_3Br/CO
α-$Fe_3(P_2O_7)_2$
$Fe_2P_2O_7$
^{57}Fe Mössbauer spectroscopy
Redox route

ABSTRACT

$FePO_4/SiO_2$ was employed for the oxidative bromination of methane (OMB) for the first time. A methane conversion of 50% and total selectivity of 96% for CH_3Br plus CO (CH_3Br:CO ≈ 1) were obtained at 570 °C. Comparison experiments were designed to investigate the roles of O_2, HBr and the catalysts. Powder X-ray diffraction (XRD), X-ray photoelectron spectroscopy (XPS), Fourier-transform infrared spectroscopy (FTIR) and ^{57}Fe Mössbauer spectroscopic studies were conducted on the catalysts. It was confirmed that the $FePO_4$ components of the fresh catalyst transformed quickly to stable active species during the induction period, and the active components of the stable catalyst have been found to consist of near-equimolar α-$Fe_3(P_2O_7)_2$ and $Fe_2P_2O_7$. The reaction over the $FePO_4/SiO_2$ catalyst was proposed to follow a redox route based on the results of comparison experiments and associated characterization.

1. Introduction

Due to the diminishing proven reserves and the increasing consumption of crude oil, utilization of methane as an alternative chemical feedstock is becoming more urgent [1]. However, as an abundant resource for chemical feedstocks, 30–60% of the natural gas reserves are classified as stranded due to the lack of infrastructure. When stranded gases are produced in the course of crude oil production, they are usually burnt at the oil-wells or vented [2,3]. It has been estimated that approximately 150 billion m^3 of natural gas has been flared or vented annually worldwide, which is equivalent to about 5% of global annual natural gas consumption [4,5]. Thus, the development of practical technologies for methane conversion at remote locations is critical for the successful utilization of these natural gas resources.

So far, the main use of methane is limited to energy production because of its highly symmetrical tetrahedral geometry and strong C–H bonds (439 kJ/mol), and the selective activation of methane presents a formidable challenge to catalysis [1]. Current industrial technologies for the production of chemicals from methane are dominated by an indirect route via syngas, i.e., methane is firstly transformed to syngas before further converting into other useful products. However, the production of syngas from methane is known to be an energy- and capital-intensive process [6]. On the other hand, direct routes for methane conversion, e.g., selective oxidation of methane to C_1-oxygenates [7] and oxidative coupling of methane to ethene [8], have shown potential advantages, but these processes remain un-commercialized because of their low methane conversions and poor product selectivities. Halogenation of methane to produce higher hydrocarbons is a lower temperature approach for methane utilization. Among the halogens, bromine has been found to be the best choice for the activation of methane [9]. The slightly exothermic reactions between bromine and methane possess the advantage that the extent of halogenation can be controlled [9]. Olah [10] has reported that bromination of methane over different supported solid super-acids could give excellent selectivity toward methyl bromide at relatively mild temperatures. Similar results have been reported recently over SBA-15-supported sulfated zirconia catalysts by Degirmenci et al. [11]. One concern of these solid super-acid catalytic systems is their long-term stability, which has not been referred to in the literature so far. It has also been reported that methane could be transformed to oxygenates and olefins in a sequential zone-flow reactor with bromine as a mediator [12–15]. However, the activation of methane in this

* Corresponding author at: Y. Ding, 457 Zhongshan Road, Dalian, Liaoning 116023, China. Fax: +86 411 84379143.
** Correspondence to: T. Zhang, 457 Zhongshan Road, Dalian, Liaoning 116023, China. Fax: +86 411 84691570.
E-mail addresses: dyj@dicp.ac.cn (Y. Ding), taozhang@dicp.ac.cn (T. Zhang).

0021-9517/$ - see front matter © 2010 Elsevier Inc. All rights reserved.
doi:10.1016/j.jcat.2010.03.011

approach was dominated by free-radical reactions occurring in the gas phase. High ratio of CH_4/Br_2 in the feed was indispensable in order to get high selectivity for methyl bromide. In a series of recent papers, Wang et al. have proposed the concept of oxidative bromination of methane (OBM) [16–18]. HBr/H_2O (a solution) and O_2 were used instead of bromine for the activation of methane in a new process. Comparing with the commercialized processes, this non-syngas route has several advantages: (1) The OBM reaction is a strongly exothermic reaction Eq. (1).

$$2CH_4 + 2O_2 + HBr \rightarrow CH_3Br + CO + 3H_2O, \quad \Delta H^0_{298\ K} = -685.8\ kJ/mol \tag{1}$$

Thus, it is an energy-saving process; (2) the OBM route is applicable for use in small- and medium-scale natural gas fields. The products of the reaction, mainly methyl bromide, could be converted immediately to useful chemicals, such as methanol, dimethyl ether and olefins [16–18], and the HBr in the effluent could be easily recycled; (3) it can provide a means for the utilization of methane that does not require a high selectivity toward a single product. The production of equimolar CH_3Br and CO is also desirable, with acetic acid as the main value-added chemical Eq. (2)

$$CH_3Br + CO + H_2O \rightarrow CH_3COOH + HBr, \quad \Delta H^0_{298\ K} = -89.0\ kJ/mol \tag{2}$$

However, it is known that a high reaction temperature and the application of noble metal components in the catalysts are necessary for the initiation of this reaction. Therefore, in order to make this reaction a potential technology for natural gas utilization, it is desirable to develop cheaper but effective catalysts that can catalyze the reaction under milder conditions.

In previous work, we have studied the OBM reaction over various non-precious metal oxide catalysts, in which rapid deactivation occurred due to the leaching of metal oxides under strong acidic reaction atmospheres [19]. $FePO_4$, well known as a cathode material for Li-ion cells [20], shows good catalytic performance in a variety of oxidation reactions, such as ammoxidation of 2-methyl pyrazine [21], oxidative dehydrogenation of isobutyric acid [22–25] and particularly partial oxidation of methane [26–31]. However, to our knowledge, no attempts have been done so far in utilizing $FePO_4$ as a catalyst for the OBM reaction. Here, we report for the first time that $FePO_4/SiO_2$ is a highly efficient and stable catalyst for the OBM reaction. In addition, possible reaction route is also described.

2. Experimental

2.1. Catalyst preparation

Bulk phase and silica-supported $FePO_4$ were prepared by co-precipitation and impregnation method, respectively, according to the literature [26]. For the bulk $FePO_4$, aqueous solutions of $Fe(NO_3)_3$ and $NH_4H_2PO_4$ (P/Fe = 1.0) were mixed thoroughly and dried at 90 °C overnight to yield a whitish-yellow paste. The precursor obtained was calcined at 600 °C for 10 h to generate the catalyst. The silica-supported $FePO_4$ catalysts were prepared by impregnating silica-gel overnight with the mixed solution mentioned above. The slurry was then dried and activated as described above for the bulk phase $FePO_4$. Powder X-ray diffraction (XRD) measurements have confirmed the successful synthesis of crystalline $FePO_4$ for the bulk phase catalyst. For the silica-supported $FePO_4$ catalysts, no diffraction patterns were detected when the loading of $FePO_4$ was less than 40 wt.%. Hereafter, the catalyst with 10 wt.% loading of $FePO_4$ was denoted as 10 $FePO_4/SiO_2$. The physical properties of the support and the as-prepared catalysts were analyzed by the N_2-adsorption–desorption method, and the results are listed in Table 1.

Table 1
Physical properties of the support and the synthesized catalysts.

Catalyst	Surface area (m^2/g)	Mesopore volume (ml/g)	Average pore size (nm)
SiO_2	385	1.09	11.4
10 $FePO_4/SiO_2$	363	1.03	11.4
$FePO_4$	6	0.06	0.5

2.2. OBM reaction evaluation

The activity measurements were performed in a specifically designed 12-mm id quartz-tube micoreactor. For rapid venting of gaseous products, the diameter was decreased to 6 mm from the middle to the bottom. The liquid feeds were introduced by a syringe. Typically, 2.0 g of catalyst was loaded in the central part of the reactor between two plugs of quartz wool. Then, quartz beads (20–40 mesh) were loaded above the catalyst bed to provide a preheated zone as well as for uniform gas distribution. In a blank test, only quartz sand was loaded. The sampling and analysis methods have been described elsewhere [19]. For most of the tests, carbon mol balances were within 100 ± 1%. Additionally, the gas hourly space velocity (GHSV) is defined as the volumetric flow rate of total inlet gas per gram of catalyst.

2.3. Characterization of catalysts

The structural properties of the samples were determined by the N_2-adsorption–desorption method, using a physical adsorption instrument (Quantachrome, USA). Specific surface area and pore volumes were determined by N_2 adsorption at 77 K after samples were pre-treated at 623 K under vacuum for 3 h. Inductively coupled plasma (ICP) experiments were performed over a Plasma-Spec-II spectrum apparatus (LEEMAN, USA). Fourier-transform infrared spectra (FTIR) were recorded with a BRUKER EQUINOX 55 Spectrometer, having a resolution of 4 cm^{-1} and using the KBr disk method.

XRD measurements of the samples were performed on a Philips X'pert MPD X-ray diffraction spectrometer equipped with a graphite monochromator and Cu Kα (40 kV, 40 mA) irradiation, covering 2θ angles between 10° and 60°.

X-ray photoelectron spectroscopy (XPS) measurements were conducted with a VG ESCALAB MK2 system, using Al Kα radiation. Binding energies were corrected using C 1s photoelectron peak at 284.6 eV as a reference. The surface composition was determined from the peak areas and sensitive factors presented by Physical Electronics [32].

^{57}Fe Mössbauer spectra of the catalysts were recorded using a Topologic 500A spectrometer and a proportional counter at room temperature. ^{57}Co(Rh) moving in a constant acceleration mode was used as radioactive source. All of the spectral analyses were conducted assuming a Lorentzian lineshape for computer folding and fitting. Accordingly, ^{57}Fe Mössbauer spectral parameters such as the isomer shift (δ), the electric quadrupole splitting (Δ), the full linewidth at half maximum (2Γ) and the relative spectral area (F) of different components on the absorption patterns were obtained. The δ values were quoted relative to α-Fe at room temperature.

It should be mentioned that the samples after each catalytic test were cooled down rapidly to room temperature under flowing nitrogen and then transferred to a desiccator. No special care was taken during the following characterization processes.

3. Results

3.1. Catalytic performance of the $FePO_4/SiO_2$ catalyst for the OBM reaction

Fig. 1 shows the time-on-stream performance of the OBM reaction over the $FePO_4/SiO_2$. It was found that the performance gradually became stable and did not show any loss of activity in the following 70 h after an induction period of approximately 30 h. CH_4 conversion of about 50% and total selectivity of 96% for CH_3Br plus CO could be obtained on a single pass, with CH_3Br/CO ratio close to 1.0. O_2 was completely consumed during the reaction course. No CO_2 has been detected, and CH_2Br_2 was the only "by-product" (less than 5%) which could be fed back to the reactor and cycled for re-proportionation with methane. This unique product distribution rendered it a promising feedstock for the production of acetic acid, as CH_3Br has been shown to be as effective as CH_3OH for carbonylation [16]. For comparison with previous results in the literature, Br atom utilization efficiency (Eff_{Br}) in a single pass is defined as Eq. (3) (based on Eq. (1) and calculated as moles of Br).

$$Eff_{Br} = \frac{CH_3Br_{out}}{HBr_{in}} \times 100\% \quad (3)$$

It was noted that Eff_{Br} of about 29% was obtained in our process. This parameter was almost doubled compared with the highest Eff_{Br} in the previous reports [19,33]. Since the OBM route requires recycle of HBr, the higher Eff_{Br} in our catalytic system makes this process even more competitive. A detailed comparison was made and summarized in Table 2.

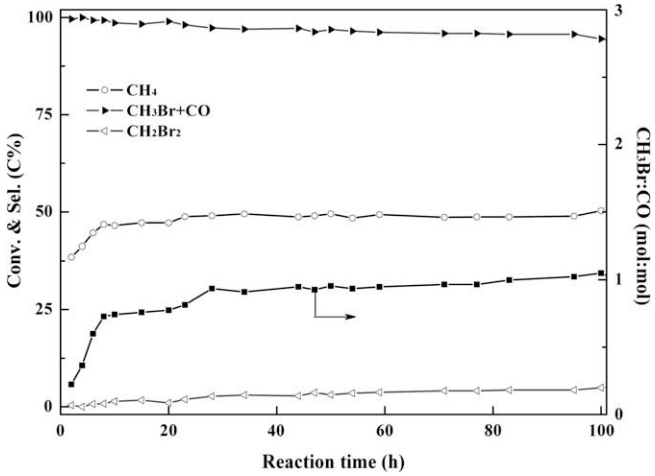

Fig. 1. Time-on-stream performance of the OBM reaction. Reaction conditions: catalyst 10 $FePO_4/SiO_2$ 2.0 g, T 570 °C, 40 wt.% HBr/H_2O 3.0 ml/h, gas flow 15 sccm (CH_4/O_2 = 2.0).

Leaching of the active components is the cause of deactivation for the catalysts during the OBM reaction [19]. The ICP analysis of the used catalysts for various reaction time has confirmed that the elemental weights of Fe and P dropped from 3.71% and 2.04% to 3.04% and 1.69%, respectively, in the first 10 h of time-on-stream. Then, they slightly decreased to 3.00% and 1.41% in the subsequent 90 h. These results demonstrated that the $FePO_4/SiO_2$ was a relatively stable and HBr-tolerant catalyst, and its reactivity increased noticeably after the reaction has run for 10 h. It was speculated that the $FePO_4$ components might transform to other phases which were more tolerant to HBr.

3.2. XPS and FTIR characterization of the fresh and used catalysts

In order to monitor the chemical states of the surface elements, XPS measurements were performed for the $FePO_4/SiO_2$ catalysts that have been operated for different reaction time, and the results are presented in Table 3. It is clear that the binding energies (B. E.) of Fe $2p_{3/2}$ shifted gradually to a lower B. E. region with reaction time, indicating a partial reduction of the $FePO_4$. Besides, calculations for the peak areas have revealed that the surface P/Fe ratio decreased slightly, but remained at above 1.09 during the reaction.

Then, the transmission IR spectra were recorded for the fresh and used catalysts, and no changes were observed between them (Fig. 2 and Table 4). It is well known that the peaks at the region between 500 and 1200 cm^{-1} correspond to the symmetric and asymmetric vibrations of the phosphate groups. It was interesting to find that a distinct band at 809 cm^{-1}, which could be attributed to asymmetrical vibrations of P–O–P groups [22,34], was detected in the fresh catalyst. This is different from the results reported by Alptekin et al. who had found that this distinct peak existed only when the fresh catalyst was employed for partial oxidation of methane [30]. This controversy could result from the differences in silica carriers, e.g., the specific surface area of the carrier used in our work is 100 m^2/g higher than that used by Alptekin. It was likely that the P–O–P groups were formed by the dehydration of

Table 3
XPS results for the fresh and used 10 $FePO_4/SiO_2$ catalysts.[a]

Reaction time (h)	B. E. (eV)[b]			P/Fe[c] (mol/mol)
	Fe $2p_{3/2}$	P 2p	Si 2p	
0	710.7	133.7	103.3	1.34
10	710.6	134.5	103.3	1.26
20	710.5	134.5	103.4	1.11
50	710.2	134.7	103.1	1.19
100	710.0	134.7	103.1	1.09

[a] Reaction conditions: catalyst 10 $FePO_4/SiO_2$ 2.0 g, T 570 °C, 40 wt.% HBr/H_2O 3.0 ml/h, gas flow 15 sccm (CH_4/O_2 = 2.0).
[b] Binding energies are reliable within ±0.3 eV.
[c] P/Fe ratios were calculated from peak areas of Fe $2p_{3/2}$ and P 2p.

Table 2
Comparison of performances of the OBM reaction over different catalysts.

Catalyst	T (°C)	GHSV (ml/(g_{cat} h))	CH_4/O_2	Liquid feeds[a] (ml/(g_{cat} h))	Conv. of CH_4%	Eff_{Br}%	Lifetime
RuNiBaLa[b]	660	300	1.0	4.0	70.0	7	Unpublished
BaO/SiO_2[c]	620	840	2.5	4.0	44.2	18	~30 h
$FePO_4/SiO_2$	570	300	2.0	1.5	49.5	29	>100 h

[a] 40 wt.% HBr/H_2O.
[b] Ref. [33].
[c] Ref. [19].

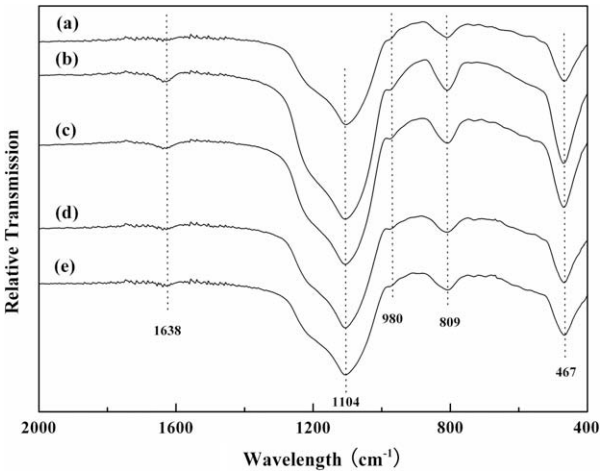

Fig. 2. Infrared spectra of the 10 $FePO_4/SiO_2$ after different reaction time: (a) fresh; (b) 10 h; (c) 20 h; (d) 50 h; and (e) 100 h.

Table 4
Assignment of IR bands in the spectra of the catalysts.

10 $FePO_4/SiO_2$		$FePO_4$	
Band (cm^{-1})	Assignment	Band (cm^{-1})	Assignment
1638	OH H_2O	1086	$\nu_{as}(PO_3)$
1104	$\nu(PO_3)$	1026	$\nu(PO_3)$
980	$\nu(PO_3)$	971	$\nu_{as}(POP)$
809	$\nu_{as}(POP)$	736	$\nu_{as}(POP)$
467	$\delta(PO_3)$	636	$\delta(PO_3)$
		594	$\delta(PO_3)$
		577	$\delta_{as}(PO_3)$
		528	$\delta_{as}(PO_3)$
		432	$\delta(PO_3)$

well-dispersed PO_3 groups on the surfaces of the silica during drying and calcining processes.

3.3. Comparison experiments on the OBM reaction

3.3.1. Comparison experiment I: effects of catalysts and reactants

One of the key considerations of present work was to understand the roles of the $FePO_4$. For such a goal, a series of comparison experiments were designed, and the results of the first comparison experiment are summarized in Table 5. It is clear that the highest methane conversion was achieved on the $FePO_4/SiO_2$ (Table 5, Entry 5), yielding CH_3Br and CO as the main products. On the other hand, the bulk phase $FePO_4$ yielded 4.5% CH_4 conversion and a lower CO selectivity. It should be mentioned that only a trace amount of methane was converted at temperatures above 600 °C in the blank test. The large contrast implied that the gaseous free-radical reactions hardly occur in the absence of a catalyst. Accordingly, we have investigated the roles of O_2 and HBr in the reaction (Table 5, Entries 2, 3 and 5). The results showed that both of them were indispensable for high methane conversion.

Table 5
Comparison experiments on the OBM reaction.[a]

Entry	Catalyst	Conversion CH_4 (%)	Selectivity (C%)		
	2.0 g		CH_3Br	CO	CH_2Br_2
1	Blank	0	0	0	0
2[b]	10 $FePO_4/SiO_2$	1.3	79.2	5.7	15.1
3[c]	10 $FePO_4/SiO_2$	2.8	0	100	0
4	$FePO_4$	4.5	71.6	13.3	15.1
5	10 $FePO_4/SiO_2$	17.1	51.2	41.3	7.5

[a] Reaction conditions: *T* 450 °C, 40 wt.% HBr/H_2O 2.0 ml/h, gas flow 10 sccm (CH_4/O_2 = 1.0).
[b] O_2 was replaced by N_2.
[c] No HBr/H_2O.

3.3.2. Comparison experiment II: bulk phase $FePO_4$ as a model catalyst

To gain further information about the phase evolution of the supported catalyst, the bulk phase $FePO_4$ was used as a model catalyst for the OBM reaction. XRD patterns in Fig. 3 revealed that $FePO_4$ was reduced completely to $Fe_2P_2O_7$ when treated in HBr alone, while phases containing mixed valences for iron, such as α-$Fe_3(P_2O_7)_2$ and an unknown *Z* phase (2θ = 30.0° and 30.4°), were detected in the catalyst after treated in the reaction atmosphere. IR spectra of the catalysts after subjected to different treatments were also presented (Fig. 4 and Table 4). Absorptions of the HBr-reduced bulk catalyst at the range of 400–1200 cm^{-1} is a typical spectrum of $Fe_2P_2O_7$ [22], and this is consistent with the XRD results. On the other hand, no distinct absorption peaks were observed in the spectrum of the bulk phase $FePO_4$ after exposure to the reaction stream. Muneyama et al. [22] have observed similar phenomena when $FePO_4$ was reduced in a stream of isobutyric acid. They have speculated that the component of this unknown phase (referred to

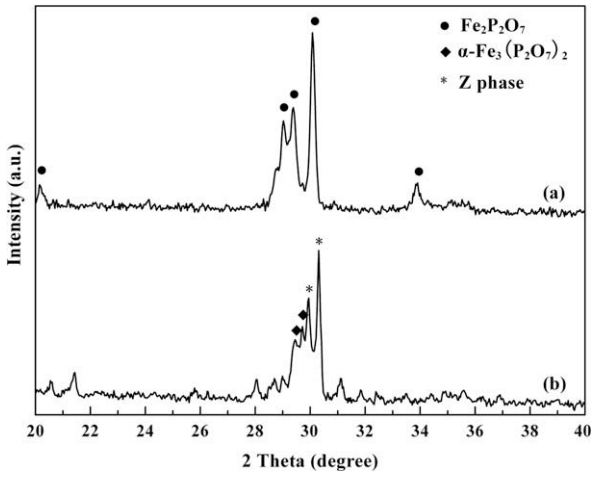

Fig. 3. XRD patterns of the catalysts treated in different reaction atmospheres for 10 h. Reaction conditions: catalyst $FePO_4$ 2.0 g, *T* 570 °C, 40 wt.% HBr/H_2O 3.0 ml/h, gas flow 15 sccm (a) CH_4/N_2 = 2.0; and (b) CH_4/O_2 = 2.0.

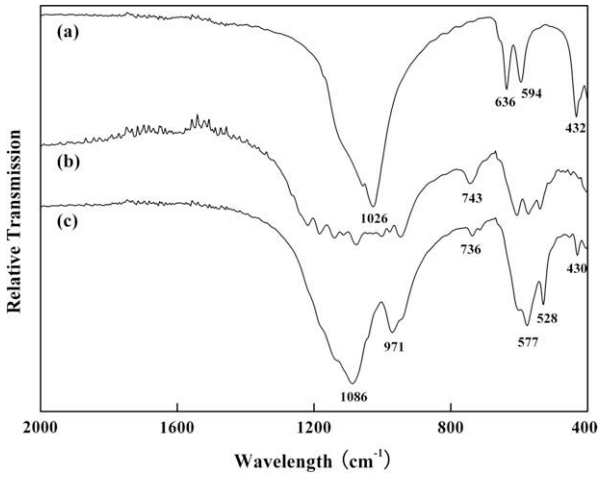

Fig. 4. Infrared spectra of the bulk phase $FePO_4$ after treated in different reaction streams at 570 °C for 10 h: (a) fresh; (b) CH_4/O_2 (2:1) 15 sccm, 40 wt.% HBr/H_2O 3.0 ml/h; (c) N_2 15 sccm, 40 wt.% HBr/H_2O 3.0 ml/h.

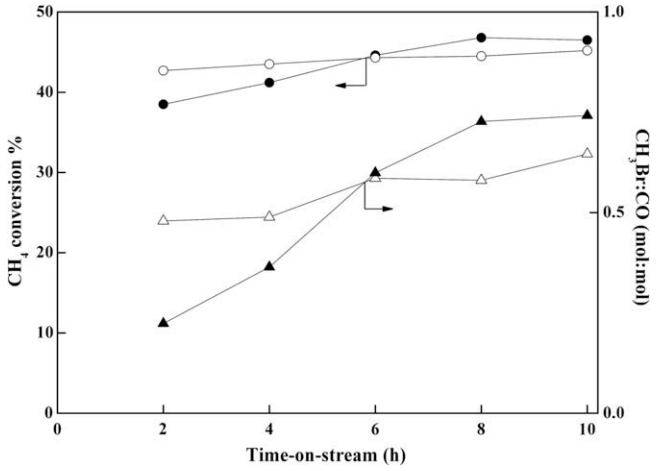

Fig. 5. Performances of the 10 $FePO_4/SiO_2$ in the OBM reaction as a function of time-on-stream. Reaction conditions: *T* 570 °C, CH_4 10 sccm, O_2 5 sccm, 40 wt.% HBr/H_2O 3.0 ml/h, catalyst 2.0 g. Filled symbols: fresh catalyst; unfilled symbols: 10 $FePO_4/SiO_2$ pre-treated in HBr/H_2O (3.0 ml/h) overnight at 570 °C.

as the *Y* phase) could be $Fe_3(P_2O_7)_2$ and/or $Fe_2P_2O_7$, because the IR spectral shape of this phase resembled somewhat that of the standard $Fe_3(P_2O_7)_2$. Their speculation was consistence with our findings in XRD results. Obviously, $FePO_4$ could not be totally reduced to $Fe_2P_2O_7$ in the reaction stream.

3.3.3. Comparison experiment III: effect of HBr pre-reduction

Fig. 5 shows the performances of the initial 10 h over $FePO_4/SiO_2$ catalysts pre-reduced by HBr and un-pre-reduced by HBr in the OBM reaction. It is obvious that the performances of HBr pre-treated catalyst showed the same trends as that of the un-pre-reduced counterpart. A similar induction period could be clearly observed, which signified a slight increase in methane conversion and a rapid increase in the ratio of CH_3Br/CO, although the increasing rate was a little slower over the pre-reduced catalyst.

3.4. ^{57}Fe Mössbauer spectroscopic studies on the OBM catalysts

3.4.1. ^{57}Fe Mössbauer spectroscopic studies on the HBr-reduced and the un-reduced FePO4 catalysts

In order to determine the chemical state and coordination of the iron species in the catalyst sample, Mössbauer spectroscopy was employed to study the HBr-reduced and the un-reduced $FePO_4$ catalysts and the results are shown in Fig. 6, with the hyperfine interaction parameters summarized in Table 6. The spectrum of the un-reduced $FePO_4$ catalyst (Fig. 6a) could be fitted into a Fe^{3+} doublet. The obtained ^{57}Fe Mössbauer parameters of δ and Δ were characteristic of ferric cations in symmetrical tetrahedral environment [30,35]. After the treatment with HBr, the spectral shape of the $FePO_4$ catalyst changed remarkably. The spectrum (Fig. 6b) could be fitted into a ferric and a ferrous doublet, indicating that the iron cations were existing in two very different chemical environments. The hyperfine interaction parameters of the main component having a relatively larger δ and Δ values are in good agreement with that of $Fe_2P_2O_7$ [25], indicating that the $FePO_4$ was reduced by HBr, which was confirmed by the XRD results. Besides $Fe_2P_2O_7$, another component in relatively small quantities (about 14.0%) was present, and the hyperfine interaction parameters were similar to that of ferric cations in a trigonal bipyramid environment [36].

3.4.2. ^{57}Fe Mössbauer spectroscopic studies on the 10 FePO4/SiO2 catalysts after different time-on-stream

Although the comparison experiments on the bulk phase catalyst have demonstrated phase transformation occurred under different treatments, the real transformation processes of the silica-supported $FePO_4$ catalyst under reaction atmosphere were largely

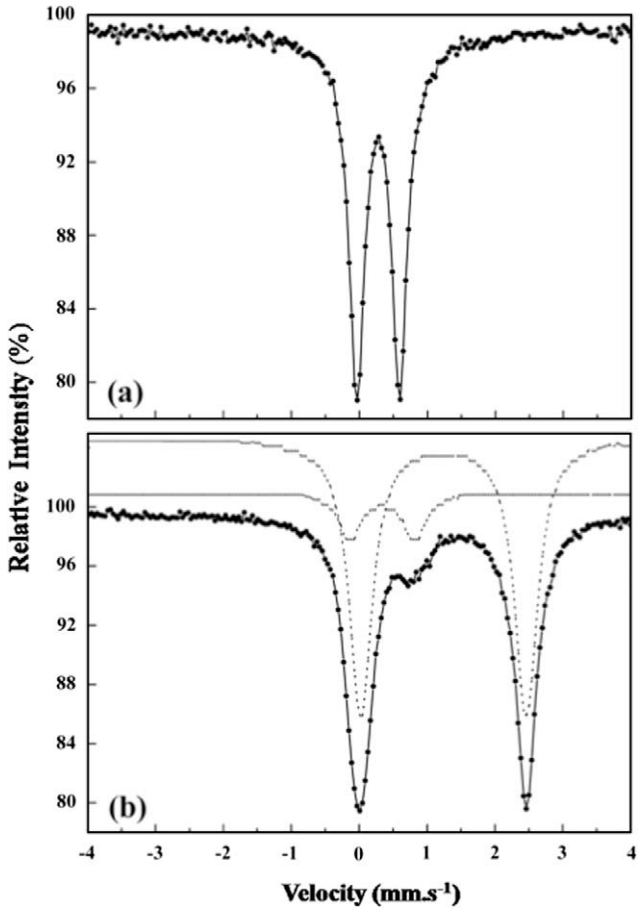

Fig. 6. Room temperature ^{57}Fe Mössbauer spetra of (a) fresh and (b) HBr-reduced $FePO_4$ catalysts.

Table 6
^{57}Fe Mössbauer parameters of the $FePO_4$ and 10 $FePO_4/SiO_2$ catalysts at room temperature.

Entry	Component	δ[a] (mm s^{-1})	Δ[b] (mm s^{-1})	2Γ[c] (mm s^{-1})	F[d](%)
1 – Fig. 6a	Fe^{3+}	0.27	0.63	0.28	100
2 – Fig. 6b	Fe^{3+}	0.34	0.95	0.39	14.0
	Fe^{2+}	1.24	2.43	0.41	86.0
3 – Fig. 7a	Fe^{3+}	0.26	1.22	0.57	45.2
	Fe^{3+}	0.27	0.69	0.48	54.8
4 – Fig. 7b	Fe^{3+}	0.27	0.69	0.54	74.7
	Fe^{2+}	1.20	2.24	0.46	25.3
5 – Fig. 7c	Fe^{3+}	0.47	0.59	0.50	38.6
	Fe^{2+}	1.22	2.49	0.45	61.4
6 – Fig. 7d	Fe^{3+}	0.47	0.58	0.43	40.4
	Fe^{2+}	1.20	2.50.	0.42	59.6
7 – Fig. 7e	Fe^{3+}	0.47	0.58	0.44	40.3
	Fe^{2+}	1.20	2.51	0.44	59.7
8 – Fig. 7f	Fe^{3+}	0.46	0.59	0.39	41.0
	Fe^{2+}	1.20	2.53	0.41	59.0
9 – Fig. 8a	Fe^{3+}	0.48	0.53	0.44	34.4
	Fe^{2+}	1.21	2.47	0.44	65.6
10 – Fig. 8b	Fe^{3+}	0.45	0.61	0.48	54.1
	Fe^{2+}	1.18	2.57	0.44	45.9

[a] Isomer shift, relative to α-Fe.
[b] Electric quadrupole splitting.
[c] Full linewidth at half maximum.
[d] Relative resonance areas of the different components of the absorption patterns.

unknown, especially when an induction period was involved. Hence, detailed studies on the phase transformations of the $FePO_4$ precursor of the $FePO_4/SiO_2$ catalyst were carried out by employing the ^{57}Fe Mössbauer spectroscopy technique. Representative Mössbauer spectra of $FePO_4/SiO_2$ catalysts after different time-on-stream are presented in Fig. 7, and the hyperfine interaction parameters are listed in Table 6.

Fig. 7a shows the Mössbauer spectrum of the fresh $FePO_4/SiO_2$ catalyst. The spectrum could be fitted into two Fe^{3+} doublets of relatively the same quantity. The quadrupole doublet with $\delta = 0.27$ mm s^{-1} and $\Delta = 0.69$ mm s^{-1} is quite similar to that of the bulk phase $FePO_4$, such that the ferric cations should be tetrahedrally coordinated with oxygen. Another doublet has a similar δ value, while the Δ value is much higher. This iron species could be ascribed to the highly dispersed ferric cations having strong interactions with the silica. On the other hand, all of the Mössbauer spetra for the used $FePO_4/SiO_2$ catalysts exhibit three absorption peaks that could be fitted into a ferric and a ferrous doublet, which implied that ferric cations were partially reduced to ferrous cations during the reaction. Obviously, the Mössbauer spectra from Fig. 7a–c changed remarkably while those from Fig. 7c–f were very similar, as can also be seen from the parameters of hyperfine interaction. Therefore, the catalyst should remain very stable after reacting for 1 h. The hyperfine interaction parameters of the ferric doublet ($\delta = 0.47$ mm s^{-1} and $\Delta = 0.59$ mm s^{-1}) in the stable catalysts are very close to the reported data of ferric cations in bulk α-$Fe_3(P_2O_7)_2$ [25], and those of the ferrous doublet ($\delta = 1.22$ mm s^{-1} and $\Delta = 2.49$ mm s^{-1}) are quite similar to the $Fe_2P_2O_7$ phase in the HBr-reduced catalyst. Since the hyperfine interaction parameters of the ferrous doublet between α-$Fe_3(P_2O_7)_2$ and $Fe_2P_2O_7$ are very close, the relative molar ratio of these two components in the sample could be estimated according to Eq. (4) without further fitting of the original patterns.

$$\alpha\text{-}Fe_3(P_2O_7)_2 : Fe_2P_2O_7 = \frac{F_{Fe^{3+}}}{(F_{Fe^{2+}} - 0.5F_{Fe^{3+}})} \quad (4)$$

Here, F is the relative intensity of iron cations listed in Table 6, and the ratio of Fe^{3+}/Fe^{2+} is 2 for α-$Fe_3(P_2O_7)_2$. It was also revealed that the ratio of α-$Fe_3(P_2O_7)_2/Fe_2P_2O_7$ changed only slightly, i.e., between 0.91 and 1.06 after 1 h's exposure in the reaction ambiance.

3.4.3. ^{57}Fe Mössbauer spectroscopic studies on the HBr-reduced 10 FePO4/SiO2 catalysts

In Section 3.3.3, the effect of HBr-reduction on the $FePO_4/SiO_2$ catalyst for the OBM reaction has been examined. A similar induction period as in the case of the fresh catalyst was observed. For a better understanding of the phase transformation process, ^{57}Fe Mössbauer spectra of the HBr-reduced $FePO_4/SiO_2$ catalysts were recorded before and after the reaction (Fig. 8 and Table 6). The Mössbauer spectrum of the HBr pre-treated $FePO_4/SiO_2$ catalyst

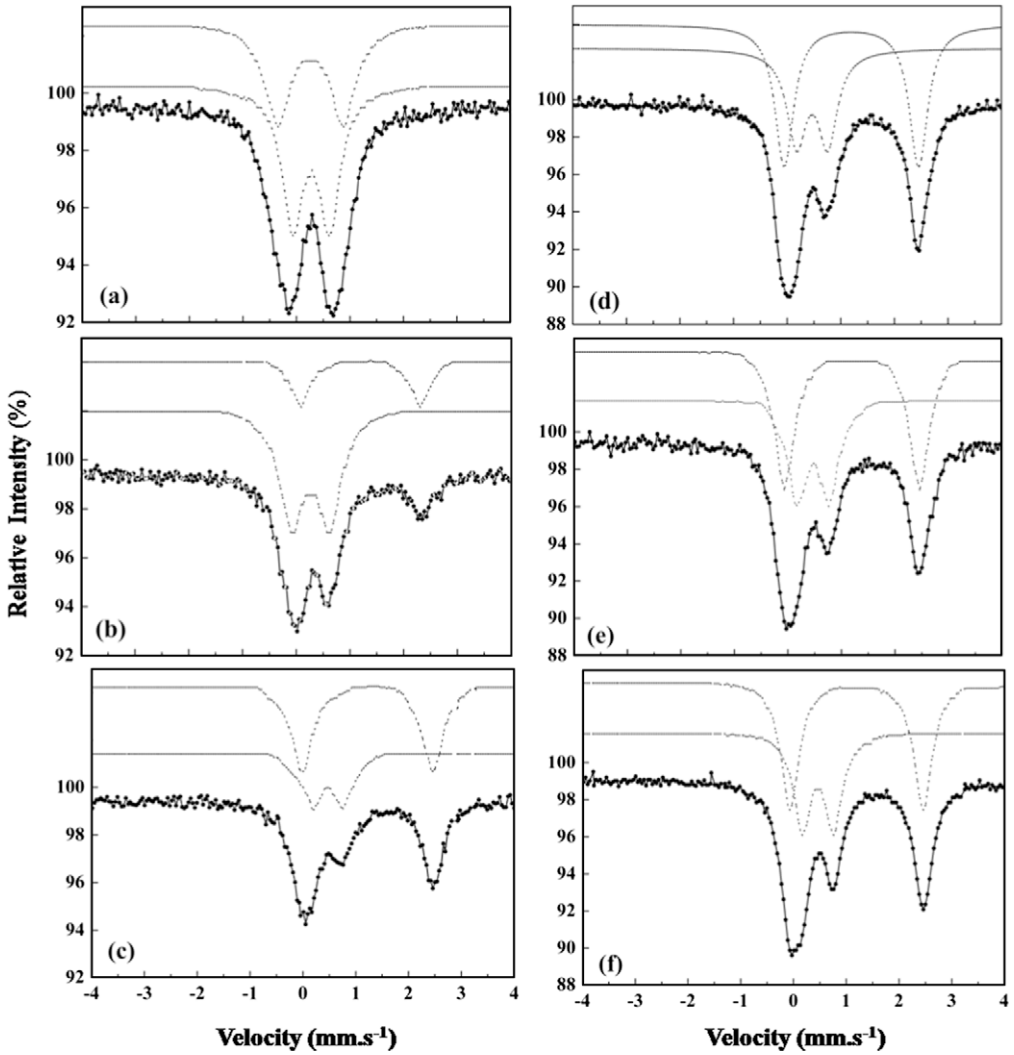

Fig. 7. Room temperature ^{57}Fe Mössbauer spetra of (a) fresh and used 10 $FePO_4/SiO_2$ catalysts for different reaction time: (b) 0.5 h, (c) 1 h, (d) 10 h, (e) 20 h and (f) 50 h.

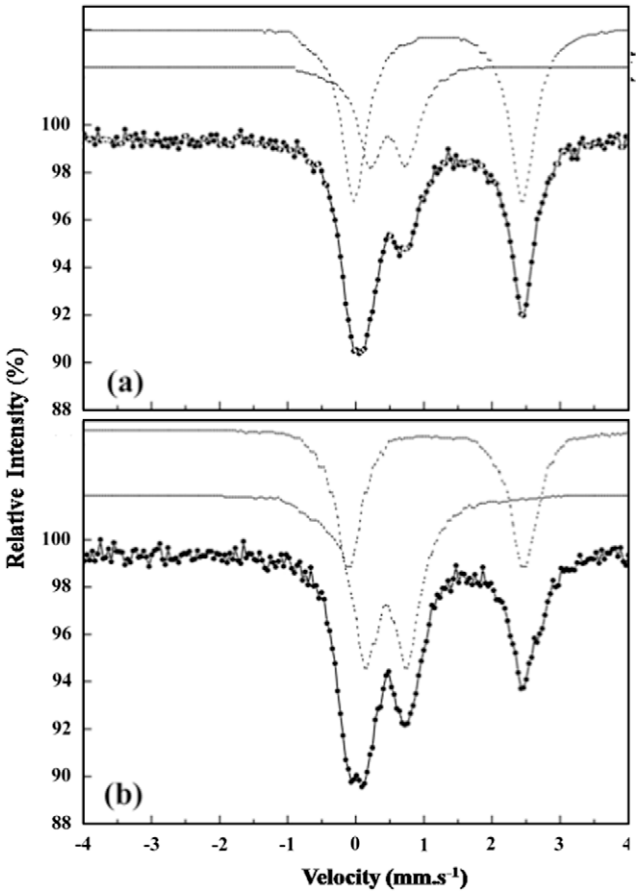

Fig. 8. Room temperature ^{57}Fe Mössbauer spetra of the HBr-reduced 10 $FePO_4/SiO_2$ catalyst (a) before and (b) after the OBM reaction.

before the reaction is shown in Fig. 8a. The spectrum could be fitted into a ferric and a ferrous doublet. The hyperfine interaction parameters of the doublets are close to those of the stable catalyst, which suggested that the initial components of the reduced sample were comprised mainly of a mixture of α-$Fe_3(P_2O_7)_2$ and $Fe_2P_2O_7$. However, the ratio of α-$Fe_3(P_2O_7)_2/Fe_2P_2O_7$ was calculated to be 0.71, that is, far less than that of the stable catalyst. It is obvious that more ferric cations could be reduced in the absence of O_2. The Mössbauer spectrum of the reduced catalyst after the OBM reaction is presented in Fig. 8b. The hyperfine interaction parameters of the two fitted doublets for this spectrum showed a slight difference to those of the reduced catalyst. The ratio of α-$Fe_3(P_2O_7)_2/Fe_2P_2O_7$ in this sample was estimated to be 2.87.

4. Discussion

4.1. Evidence for a redox route

The OBM reaction mediated by metal oxide catalysts has been studied only for a few years, and fundamental mechanistic investigations are rarely investigated owing to the presence of HBr/Br_2 as well as the complexity of the system. It was observed that the effluents leaving the quartz reactor were red–brown in color at relatively low reaction temperatures ($T < 500$ °C), suggesting the presence of bromine in the products. On the basis of established chemistry, the formation of bromine should involve the generation of bromine radicals (Br^*), which, we suppose, are the active species for methane activation in this reaction. It is speculated that the OBM reaction proceeds in a strong reductive atmospheres basing on the following two facts: (1) Rh^0 was found in a used Rh_2O_3/SiO_2 catalyst [37]; (2) crystalline $BaSi_2$ was detected in a BaO/SiO_2 catalyst after the reaction [19]. Therefore, any catalyst with strong redox ability might be a good candidate for this reaction, as is the case of the iron phosphate catalyst.

Compared with the reported OBM systems, the initial temperature of this system was much lower. Strikingly, we have observed appreciable methane conversion over the $FePO_4/SiO_2$ even at a temperature as low as 430 °C. On the other hand, other researchers have reported on the use of $FePO_4$ for partial oxidation of methane at a temperature range of 400–600 °C, but in these cases, methane conversion rarely exceeded 10%, and the selectivity toward CO_x ($x = 1, 2$) was significant [26,29–31]. These facts undoubtedly suggested the chemical involvement of our catalytic system was quite different from that of the partial oxidation of methane.

The first comparison experiment on the role of the different reactants revealed that maximum methane conversion could only be obtained in the presence of both HBr and O_2 over the $FePO_4/SiO_2$ catalyst. Based on these observations, we have speculated that the participation of the $FePO_4/SiO_2$ opened up a new reaction avenue in the presence of O_2 and HBr. Thus, the OBM reaction could proceed at much lower temperatures. The second comparison experiment on the $FePO_4$ model catalyst further confirmed that the $FePO_4$ could be completely reduced to $Fe_2P_2O_7$ by HBr alone, whereas it could only be partially reduced in the OBM reaction atmosphere. This distinction is strong evidence showing that the OBM reaction proceeds via a redox route. It is well known that oxy-chlorination reactions over copper-based catalysts are driven by the Cu^+/Cu^{2+} redox couple [38,39]. Considering the similarities of the reaction systems between the OBM and oxy-chlorination reactions, one might speculate that the functions of $FePO_4$ in the present system, to some extent, are the same as those of CuCl in the oxy-chlorination reaction systems.

4.2. Insight into the active phases

In Section 3.4.2, ^{57}Fe Mössbauer spectroscopic studies on the used catalysts have demonstrated that typical stable components of the $FePO_4/SiO_2$ were comprised of near-equimolar α-$Fe_3(P_2O_7)_2$ and $Fe_2P_2O_7$. It should be noted that the ratios of P/Fe calculated from the stable catalysts were around 1.24, which is very close to the surface elemental ratio of P/Fe (about 1.20) derived from the XPS determination but much higher than those determined in the ICP analyses (P/Fe = 0.85–1.00).

Although the phase transformation processes from the $FePO_4$ precursor to the final stable components (α-$Fe_3(P_2O_7)_2/Fe_2P_2O_7 \approx 1$) were almost completed in the initial 1 h, as can be clearly seen in Table 6, it was worthy to emphasize that the evolution was not a single simple process. The transformation from the fresh catalyst to the stable one is not due to the transformation of one well-defined crystalline material into another, rather, it involves two topotactic transformations that took place very quickly after heating in the reaction stream. The coordination environment of ferrous cations in Fig. 7b with $\delta = 1.20$ mm s^{-1} and $\Delta = 2.24$ mm s^{-1} cannot be well defined yet. Apparently, the species have a similar δ value when compared to the stable catalyst, but the Δ value is much smaller. Thus, we can hypothesize that the evolutions might involve certain intermediate species. By comparing with Figs. 7a and 7b, it was found that the bulk $FePO_4$-like component still existed, while that of the counterpart disappeared after running for half an hour in the reaction stream. When the reaction time was prolonged to 1 h, even the bulk $FePO_4$-like component vanished. It is evident that crystalline-like $FePO_4$ was a more stable phase in the fresh catalyst. By carefully analyzing the hyperfine interaction parameters of Figs. 7a–c, it was not difficult to find that the transformation processes of α-$Fe_3(P_2O_7)_2$ and $Fe_2P_2O_7$ might

proceed in two different ways. It seemed that the α-$Fe_3(P_2O_7)_2$ was most likely derived from the crystalline-like $FePO_4$, while the $Fe_2P_2O_7$ was most likely transformed from the $FePO_4$ that was interacting strongly with the SiO_2 support. Besides, the evolution of the $Fe_2P_2O_7$ was prior to the transformation of the α-$Fe_3(P_2O_7)_2$. It should be noted that the relative intensity of the iron species in different coordination environments in the fresh catalyst is close to 1, as can be seen in Table 6. This is in accord with the ratio of α-$Fe_3(P_2O_7)_2$/$Fe_2P_2O_7$ in the stable catalyst, regardless of iron leaching during the reactions.

The third comparison experiment revealed that the OBM reaction over both the un-pre-reduced and the HBr-pre-treated $FePO_4/SiO_2$ catalysts went through similar induction periods. Therefore, it is very likely that both the un-pre-reduced and the HBr-pre-treated $FePO_4/SiO_2$ catalysts could transform to more active phases after a contact with the reaction atmosphere. ^{57}Fe Mössbauer spectroscopic studies on the used catalysts have demonstrated that the $FePO_4$ could completely transform to the α-$Fe_3(P_2O_7)_2$ and $Fe_2P_2O_7$ in the reaction stream. It is also evident that the $Fe_2P_2O_7$ could be converted to α-$Fe_3(P_2O_7)_2$ after re-treated by the OBM reaction, as the ratio of α-$Fe_3(P_2O_7)_2$/$Fe_2P_2O_7$ increased from 0.71 to 2.87 when the HBr-pre-treated $FePO_4/SiO_2$ catalyst was reacted for 10 h. It is noteworthy that the ratio of α-$Fe_3(P_2O_7)_2$/$Fe_2P_2O_7$ in this used catalyst is much higher than that of the stable catalyst, which implies that the catalyst might be in a transient state. If this speculation is true, then it makes sense for the existence of a reverse evolution from α-$Fe_3(P_2O_7)_2$ to $Fe_2P_2O_7$. Although the experimental results of the ^{57}Fe Mössbauer spectroscopic studies for the HBr-reduced $FePO_4/SiO_2$ catalysts are not compelling to demonstrate that the reverse evolution has occurred indeed, it is very probable that dynamic transformations between α-$Fe_3(P_2O_7)_2$ and $Fe_2P_2O_7$ have proceeded in the stable catalyst, as the reaction consisted of two entirely different ambiances (i.e., oxidative and reductive) with regard to the involvements of O_2 and HBr in the system.

The most active phase of the stable catalyst could be α-$Fe_3(P_2O_7)_2$, which is composed of three face-sharing FeO_6 octahedra clusters. It has been reported that such a configuration can facilitate the generating of intervalency for the Fe^{3+}/Fe^{2+} redox couple during catalytic reactions, thus imposing a limitation to electron hopping between the iron cations [40,41]. For the formation of α-$Fe_3(P_2O_7)_2$, excess phosphorus with respect to the stoichiometry of $FePO_4$ (P/Fe = 1.0) was deemed necessary [22]. The XPS results in Table 4 implied a phosphorus enrichment on the surface of the supported catalyst, rendering it possible for the formation of the α-$Fe_3(P_2O_7)_2$.

4.3. Reaction route

From the observations of comparison experiments I and II, it is apparent that the OBM reaction over $FePO_4/SiO_2$ proceeds via a redox path. The results of these experiments also implied the importance of reaction ambiances for methane conversion and phase evolutions, as confirmed by combined spectroscopic studies. It should be noted that the ratios of CH_3Br/CO kept increasing during the induction periods for both the untreated and the HBr pre-treated $FePO_4/SiO_2$ catalysts, which suggested that both Fe^{3+} and Fe^{2+} might be the active sites for the oxidation of bromomethanes. This speculation is in accord with our previous point of view that the presence of a solid catalyst would be favorable for the deep oxidation of bromomethanes during the OBM reaction [19].

In light of the above-mentioned evidence, a tentative redox route was proposed for the OBM reaction catalyzed by silica-supported iron phosphate catalyst, as described in Scheme 1. First, HBr can be oxidized by Fe^{3+} to highly active radicals-Br^*, with the reduction of the Fe^{3+} to Fe^{2+}. The active Br^* radicals can then attack methane to produce bromomethanes, which are further oxidized to CO in the presence of solid catalysts and O_2. Finally, the consumed Fe^{3+} can be replenished by the re-oxidation of Fe^{2+} to complete the redox cycle.

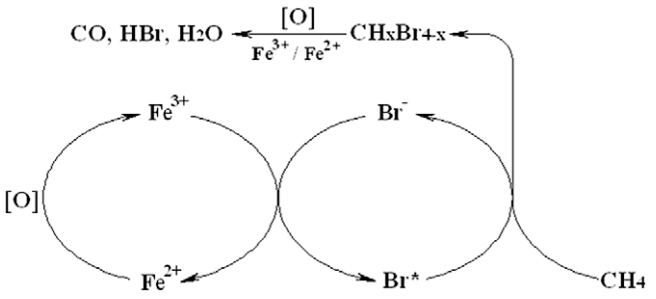

Scheme 1. A tentative redox route for the OBM reaction over the $FePO_4/SiO_2$ catalyst. *Note*: [O] could be gaseous or lattice oxygen. x = 1, 2 or 3.

5. Conclusions

We have demonstrated that an inexpensive, effective and stable silica-supported iron phosphate catalyst can be used for the OBM reaction. High methane conversion and excellent product distribution were achieved at 570 °C and under 1 atm. It was demonstrated that $FePO_4/SiO_2$, which is functioning in a completely different chemistry when compared with metal oxides catalysts, could initiate the reaction at much lower temperatures. ^{57}Fe Mössbauer spectroscopic studies have confirmed that the active species in the stable catalyst was comprised of near-equimolar α-$Fe_3(P_2O_7)_2$ and $Fe_2P_2O_7$. It was speculated that dynamic transformations between α-$Fe_3(P_2O_7)_2$ and $Fe_2P_2O_7$ might proceed in the stable catalyst during the OBM reaction, and α-$Fe_3(P_2O_7)_2$ was supposed to be the most active phase. Besides, we have proposed that the OBM reaction over the $FePO_4/SiO_2$ catalyst was dominant by a redox route, as confirmed by a series of comparison experiments and catalyst characterizations using XRD, XPS and ^{57}Fe Mössbauer spectroscopy.

Acknowledgments

This work was financially supported by the Ministry of Science and Technology of China (2005CB221406). The authors would like to express their sincere gratitude to all those who contributed to this research.

References

[1] R.H. Crabtree, Chem. Rev. 95 (1995) 987.
[2] S. Romanow, Hydrocarbon Process. 80 (2001) 11.
[3] F. Thackeray, G. Leckie, Pet. Econ. 69 (2002) 10.
[4] Reducing the Gas Burning, World Bank Weekly Update, June 26, 2006.
[5] BP Statistical Review of World Energy, British Petroleum Co., London, 2006.
[6] J.H. Lunsford, Catal. Today 63 (2000) 165.
[7] B.L. Conley, W.J. Tenn III, K.J.H. Young, S.K. Ganesh, S.K. Meier, V.R. Ziatdinov, O. Mironov, J. Oxgaard, J. Gonzales, W.A. Goddard III, R.A. Periana, J. Mol. Catal. A: Chem. 251 (2006) 8.
[8] J.H. Lunsford, Angew. Chem. Int. Ed. 34 (1995) 970.
[9] V. Degirmenci, D. Uner, A. Yilmaz, Catal. Today 106 (2005) 252.
[10] G.A. Olah, Acc. Chem. Res. 20 (1987) 422.
[11] V. Degirmenci, A. Yilmaz, D. Uner, Catal. Today 142 (2009) 30.
[12] X.P. Zhou, A. Yilmaz, G.A. Yilmaz, I.M. Lorkovic, L.E. Laverman, M. Weiss, J.H. Sherman, E.W. Mcfarland, G.D. Stucky, P.C. Ford, Chem. Commun. 18 (2003) 2294.
[13] I.M. Lorkovic, A. Yilmaz, G.A. Yilmaz, X.P. Zhou, L.E. Laverman, S. Sun, D.J. Schaefer, M. Weiss, M.L. Noy, C.I. Cutler, J.H. Sherman, E.W. Mcfarland, G.D. Stucky, P.C. Ford, Catal. Today 98 (2004) 317.
[14] I.M. Lorkovic, M. Noy, M. Weiss, J. Sherman, E. Mcfarland, G.D. Stucky, P.C. Ford, Chem. Commun. 5 (2004) 566.

[15] A. Breed, M.F. Doherty, S. Gadewar, P. Grosso, I.M. Lorkovic, E.W. Mcfarland, Catal. Today 106 (2005) 301.
[16] K.X. Wang, H.F. Xu, W.S. Li, X.P. Zhou, J. Mol. Catal. A: Chem. 225 (2005) 65.
[17] K.X. Wang, H.F. Xu, W.S. Li, C.T. Au, X.P. Zhou, Appl. Catal. A: Gen. 304 (2006) 68.
[18] Z. Liu, L. Huang, W.S. Li, F. Yang, C.T. Au, X.P. Zhou, J. Mol. Catal. A: Chem. 273 (2007) 14.
[19] R. Lin, Y. Ding, L. Gong, J. Li, W. Chen, L. Yan, L. Yuan, Appl. Catal. A: Gen. 353 (2009) 87.
[20] A.K. Padhi, K.S. Nanjundaswamy, C. Masquelier, S. Okada, J.B. Goodenough, J. Electrochem. Soc. 144 (1997) 1609.
[21] P. Nagaraju, Ch. Srilakshmi, Nayeem Pasha, N. Lingaiah, I. Suryanarayana, P.S. Sai Prasad, Catal. Today 131 (2008) 393.
[22] E. Muneyama, A. Kunishige, K. Ohdan, M. Ai, J. Catal. 158 (1996) 378.
[23] M. Ai, K. Ohdan, Appl. Catal. A: Gen. 180 (1999) 47.
[24] P. Bonnet, J.M.M. Millet, C. Leclercq, J.C. Védrine, J. Catal. 158 (1995) 128.
[25] J.M.M. Millet, Catal. Rev. – Sci. Eng. 40 (1998) 1.
[26] Y. Wang, K. Otsuka, J. Catal. 155 (1995) 256.
[27] Y. Wang, K. Otsuka, J. Mol. Catal. A: Chem. 111 (1996) 341.
[28] Y. Wang, K. Otsuka, Appl. Catal. A: Gen. 222 (2001) 145.
[29] Y. Wang, X. Wang, Z. Su, Q. Guo, Q. Tang, Q. Zhang, H. Wan, Catal. Today 93–95 (2004) 155.
[30] G.O. Alptekin, A.M. Herring, D.L. Williamson, T.R. Ohno, R.L. McCormick, J. Catal. 181 (1999) 104.
[31] R.L. McCormick, G.O. Alptekin, D.L. Williamson, T.R. Ohno, Top. Catal. 10 (2000) 115.
[32] J.H. Scofield, J. Electron Spectrosc. 8 (1976) 129.
[33] K.X. Wang, H.F. Xu, S.W. Li, X.P. Zhou, CN Patent 1 (724) (2005) 503.
[34] A. Annapragada, E. Gulari, J. Catal. 123 (1990) 130.
[35] J.M.M. Millet, C. Virely, M. Forissier, P. Bussiere, J.C. Vedrine, Hyperfine Interact. 46 (1989) 619.
[36] M.R. De Guire, T.R.S. Prasanna, G. Kalonji, R.C. O'Handley, J. Am. Ceram. Soc. 70 (1987) 831.
[37] F. Liu, Z. Liu, W.S. Li, T.H. Wu, X.P. Zhou, Catal. Lett. 124 (2008) 226.
[38] A.J. Rouco, J. Catal. 157 (1995) 380.
[39] E. Peringer, S.G. Podkolzin, M.E. Jones, R. Olindo, J.A. Lercher, Top. Catal. 38 (2006) 211.
[40] R.K. Grasselli, J. Burrington, Adv. Catal. 30 (1981) 133.
[41] J.C. Védrine, G. Goudurier, J.M.M. Millet, Catal. Today 33 (1996) 3.